



1
2
3
4

AN INVESTIGATION OF HELICOPTER
FUSELAGE NORMAL MODES OF VIBRATION

A. I. SELMY*

ABSTRACT

This paper describes an experimental study to compute the normal modes of vibrations of helicopters. The work presented herein details the normal modes characteristics between 5Hz and 50Hz of a developed helicopter. The Lynx helicopter airframe was used as the test aircraft. Each mode shape was recorded at 121 monitoring points on the airframe in the vertical, lateral and fore-and-aft directions. Complex response plots were obtained for each mode shape and the modal damping factors were estimated. The results of the experimental investigations were compared with a theoretical finite element modelling analysis. Good agreement between the finite element analysis and the experimental natural frequencies and mode shapes were obtained.

THEORETICAL INVESTIGATION OF THE NORMAL MODES

When all parts of a linear system are oscillating in phase with one frequency, such a state of motion is called normal mode or principle mode of vibration. Thus in the normal mode all parts of the system are oscillating in such a manner that they reach maximum displacements simultaneously and pass their equilibrium points simultaneously. The shape of each normal mode is fixed for a given system and is independent of the magnitude, frequency or location and direction of the applied external forces.

In the analysis of the airframe vibration it is common practice to consider the airframe as a linear system with proportional hysteretic damping. The hysteretic damping is assumed to be proportional to displacement i.e the damping force is proportional to the spring force but 90° out of phase with it.

When a linear system with proportional hysteretic damping is subjected to a set of sinusoidal forces the equation of motion in one mode may be written as:

$$M \ddot{x}(t) + (k + iH) \cdot x(t) = F e^{i\omega t} \quad (1)$$

5

* Doctor Engineer, Research and Development Sector, Arab British Helicopter Company, Arab Organization for Industrialization.

Assuming a solution of $x(t) = x e^{i\omega t}$ and substituting into Eq. (1) and removing the time dependence so:

$$- \omega^2 M + (k + iH) x = F \quad (2)$$

$$x = X_{\text{REAL}} + iX_{\text{IMAGINARY}} \quad (3)$$

Substituting Eq. (3) into Eq. (2) and equating real and imaginary parts, then,

$$\left. \begin{aligned} (k - \omega^2 M) X_R - H X_I &= F \\ H X_R + (k - \omega^2 M) X_I &= 0 \end{aligned} \right\} \quad (4)$$

It is assumed that the mass, stiffness and damping matrices are symmetric and positive definite. It is required to show that for any forcing frequency ω there exists a force set such that all elements of the displacement vector X are mutually in phase. The analysis is developed for two cases as follows:

CASE 1: When the forcing frequency is a natural frequency of the undamped system. Thus there exists a real non-trivial vector Z such that:

$$(k - \omega^2 M) = 0 \quad (5)$$

This suggests a monophasic solution to Eq. (4), namely:

$$\left. \begin{aligned} X_R &= 0 \\ X_I &= Z = -F/H \end{aligned} \right\} \quad (6)$$

CASE 2: When ω is not a root of $\det(k - \omega^2 M) = 0$. Let $S = (k - \omega^2 M)$, then S is symmetric and non singular and Eq. (4) is now:

$$\left. \begin{aligned} S X_R - H X_I &= F \\ H X_R + S X_I &= 0 \end{aligned} \right\} \quad (7)$$

If we assume that the response to be monophasic, there will exist a phase (α) such that:

$$X_R = -X_I \tan \alpha \quad (8)$$

Substituting Eq. (8) into Eq. (7) gives:

$$(S - H \tan \alpha) X_I = 0 \quad (9)$$

$$- (S \tan \alpha + H) X_I = F \quad (10)$$

Then, $S^{-1} H X_I = \cot \alpha X_I$ from Eq. (9).

A possible solution to Eq. (9) and Eq. (10) is when:

$\cot \alpha$ is an eigenvalue of $S^{-1} H$

X_I is an eigenvector of $S^{-1} H$

$$F = - (S \tan \alpha + H) X_I$$

Since S is symmetric and non singular and H is symmetric and positive definite, then X_I and $\cot \alpha$ are real. Since there are in general "n" eigenvalues of $S^{-1} H$, then at any frequency "w" there are "n" possible force sets which produce a monophase.

Equation (6) shows that when "w" is a natural frequency of the undamped system, the displacement vector, which is in quadrature with the excitation, corresponds to the eigenvector of the undamped system. This leads to the following response criterion used as the basis for the normal mode experiments:

"For a linear system with proportional hysteretic damping, excited by a set of monophase harmonic forces, a sufficient condition for the response of the system to be a normal mode is that the displacement vector be in quadrature with the excitation".

EXPERIMENTAL INVESTIGATIONS OF NORMAL MODES

Structural State:

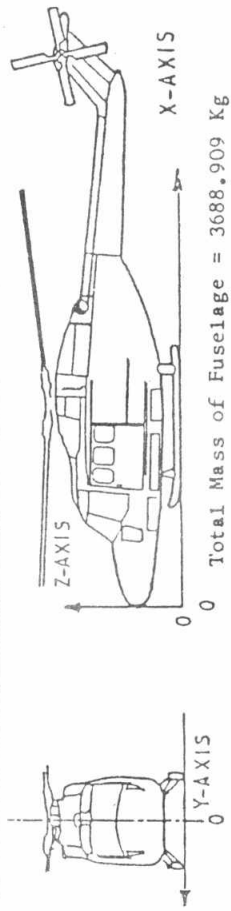
The aircraft was suspended from an overhead gantry by a heavy - duty rubber rope attached to the rotor head. This gave an approximately free-free condition as the suspension modes were of low frequency when compared with the elastic modes of the airframe. The total mass of the fuselage was equal to 3689.0 Kg as shown in Fig. 1 which shows the co-ordinates and mass of the monitoring points. There were 121 monitoring/measurement points on the airframe as shown in Fig. 2. These points were uniformly distributed throughout the structure and included all large mass items.

The main rotor blades, the tail rotor, radio, batteries, pilots, instruments, servo jacks, cabin doors and pilots doors were all removed and represented by dummy masses. Tailboom stiffening struts were also used. These struts supplement the stiffness of the tailcone/tailpylon joint and are pretensioned in order to tune the vibration characteristics.

Isolation and Measurement of Normal Modes:

The test apparatus was designed to provide multipoint excitations where an array of up to 5 vibrators with their frequency and force output was manually controlled. Each vibrator is freely suspended from a mobile support and may transmit independent forces to any point on the structure. The testing set-up was equipped with channels, each one consists of a mobile triaxial accelerometer, a charge amplifier, an integrator and an oscilloscope. Note that the several exciters are operating in parallel

Pos.	X (mm)	Y (mm)	Z (mm)	Mass (Kg)	Pos.	X (mm)	Y (mm)	Z (mm)	Mass (Kg)
75	7305	-305	1750	2.357	76	7305	-270	1330	2.158
77	7895	-225	1730	9.482	78	7895	-225	1320	9.202
79	8635	-195	1650	8.035	80	8635	-195	1295	7.735
81	9475	-175	1570	8.872	82	9475	-175	1270	6.263
83	10020	-170	1480	4.053	84	10020	-170	1265	4.053
85	10565	-188	1420	11.575	86	4705	-305	2450	17.650
87	11015	-105	1430	1.640	88	5685	-305	2400	17.650
89	4375	470	2180	33.080	90	3655	470	2195	25.201
91	3655	-470	2195	25.389	92	11635	-115	2300	1.173
93	4375	-470	2180	31.840	94	2665	-1120	70	31.126
95	4845	-1120	70	48.209	96	2235	370	2320	3.643
97	3485	200	2545	38.357	98	4035	450	2530	95.310
99	4540	305	2470	68.401	100	4705	420	2340	34.060
101	5185	500	2230	101.010	102	5685	480	2170	33.910
103	5685	-480	2170	51.055	104	5185	-500	2230	100.470
105	4705	-420	2340	51.050	106	4540	-305	2470	68.401
107	4035	-450	2530	101.204	108	3485	-200	2545	38.557
109	2235	-370	2320	3.727	110	11835	-255	2530	44.540
111	4035	1070	2830	122.500	112	5105	0	2830	122.500
113	4035	-1070	2830	122.500	114	2965	0	2830	122.500
115	2225	-460	820	48.927	116	2225	460	820	41.142
117	2280	-497	1630	26.795	118	2280	497	1630	26.795
119	1775	-530	1130	57.500	120	1775	530	1130	57.500
121	11605	0	2590	30.790					



Pos.	X (mm)	Y (mm)	Z (mm)	Mass (Kg)	Pos.	X (mm)	Y (mm)	Z (mm)	Mass (Kg)
1	12470	260	2430	0.365	2	12335	960	2420	4.500
3	12090	1730	2410	0.365	4	11910	260	2450	0.365
5	11910	960	2440	4.500	6	11910	1730	2430	0.365
7	11765	75	2150	2.345	8	11635	115	2300	1.673
9	11545	75	1820	1.910	10	11345	140	2100	4.860
11	11325	70	1720	2.05	12	11168	120	1920	2.05
13	11015	105	1430	1.320	14	10935	130	1730	5.59
15	10565	188	1420	11.575	16	10715	0	1180	6.330
17	10020	170	1480	4.052	18	10020	170	1265	4.053
19	9475	175	1570	9.122	20	9475	175	1270	6.262
21	8635	195	1650	8.035	22	8635	195	1295	7.735
23	7895	225	1730	9.533	24	7895	225	1320	9.193
25	7305	305	1750	2.343	26	7305	270	1330	2.143
27	6445	440	1770	7.945	28	6445	440	1150	13.148
29	6445	0	840	17.620	30	5735	585	1790	19.133
31	5735	585	1000	27.093	32	4855	717	1980	40.287
33	4855	767	1385	18.759	34	4855	742	810	15.499
35	4205	795	2050	38.801	36	4205	845	1420	142.046
37	4205	815	770	97.486	38	3605	827	2070	23.531
39	3605	887	1440	8.412	40	3605	862	820	84.608
41	3065	805	2000	12.550	42	3065	870	725	59.180
43	2175	827	2070	6.510	44	2155	887	1490	3.868
45	2135	862	835	30.129	46	1705	805	2130	11.500
47	1465	870	1220	14.880	48	925	735	840	48.142
49	1370	0	2130	3.830	50	955	0	1535	51.670
51	4845	1120	70	48.449	52	2665	1120	70	31.126
53	185	0	820	62.040	54	925	-735	840	57.428
55	1465	-870	1220	12.850	56	1705	-805	2130	11.500
57	2175	-827	2070	6.580	58	2155	-887	1490	3.932
59	2135	-862	835	35.217	60	3065	-870	725	61.404
61	3065	-805	2000	12.890	62	3605	-827	2070	24.309
63	3605	-887	1440	8.458	64	3605	-862	820	83.526
65	4205	-815	770	100.120	66	4205	-845	1420	141.964
67	4205	-795	2050	38.903	68	4855	-717	1980	41.643
69	4855	-767	1385	18.041	70	4855	-742	810	15.521
71	5735	-585	1790	19.487	72	5735	-585	1000	31.157
73	6445	-440	1770	8.367	74	6445	-440	1150	12.252

Fig. 1. Co-ordinates and mass of monitoring points.

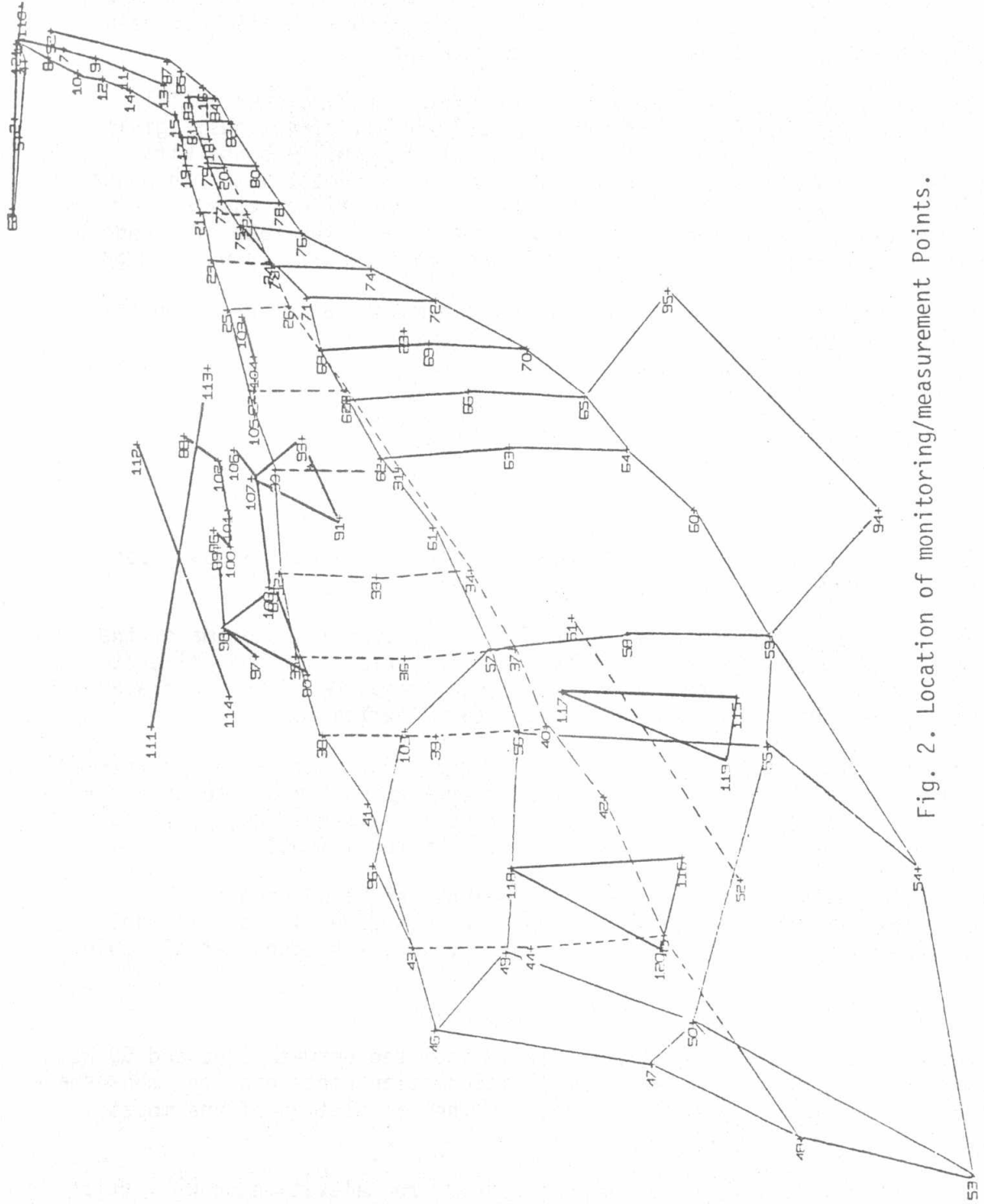


Fig. 2. Location of monitoring/measurement Points.

that are driven from individual power amplifiers and a common exciter controller. Because the oscillator signal is used as the force reference it is necessary to ensure that there is negligible phase shift between oscillator signal and excitation force. Also, phase shift have been eliminated from the power amplifiers and vibrators.

Each mode shape was recorded using a triaxial accelerometer at 121 points in the vertical, lateral and fore and aft directions, giving a response vector of order 363. Complex plotting of response with change of frequency was achieved by splitting the signal into "in phase" and quadrature components. Modal damping factor (Q) was assessed by two techniques for each mode. Two methods were used: the rate of change of phase with frequency around the resonance and the half - power method.

The mathematical expressions for the modal damping factor based on the stated two methods are respectively given by:

$$Q_A = w_n \cdot \frac{\pi}{360} \cdot \left(\frac{d\theta}{dw} \right)_{w \rightarrow w_n}$$

$$Q_B = \frac{w_n}{\Delta w}$$

Where Δw is the frequency difference between the half - power points where the amplitude is 0.707 of the peak amplitude.

Prior to the isolation of the normal modes an overall panorama of the sensitive frequencies for the dynamic characteristic of the helicopter was achieved by recording the complex frequency response of the airframe, at a number of positions, using a single point excitation.

The excitation of a normal mode of vibration of the airframe requires the finding of monophasic sinusoidal force distribution and a frequency for which a monophasic response occurs throughout the structure, with the displacement response in quadrature with the force input.

The acceptability or otherwise of each mode was based upon the characteristic phase - lag criterion with, in general, an allowable phase error of $\pm 10^\circ$ in total in phase velocity response at all points.

RESULTS AND DISCUSSION

Eleven normal modes were experimentally isolated between 5 Hz and 50 Hz. For each mode shape, a set of modal information concerning the mode shape, the complex frequency response plot and the calculation of the modal damping factor was obtained.

In the experimentally measured mode shape, the elevation shows vertical and fore and aft deflections viewed from the port side. The plan shows lateral and fore - and - aft movement of the structure looking from above. The tailplane has monitoring points along its leading and trailing edges. All sectional views and the aft view are shown looking forward. The force

6

distribution required to excite each mode is shown on the mode shape. The deflected and undeflected shapes of the airframe are shown by the solid and dotted lines respectively. Where there were direct comparisons between the Finite Element analysis and the experimental modes, the experimental values of damping were used as the damping values for the Finite Element mode. The deflections in the shake test were normalized to give a maximum deflection of one metre.

Table 1 shows the finite element and experimental mode shape comparisons and also shows the calculated damping values. As an illustration for the experimental results, only the 6.607 Hz mode and the 13.789 Hz mode are included as shown in Fig. 3 and Fig. 4 respectively. The estimation of the damping factors from experiments was dependent on modal purity and every care should be taken to ensure that all monitoring points fall within the phase tolerance which was $\pm 10^\circ$.

CONCLUSIONS

Eleven normal modes of Lynx helicopter between 5 Hz and 50 Hz have been experimentally isolated. Comparisons between the shake tests and the finite element results have shown good agreement for frequencies and mode shapes. However, it can be seen that the finite element analysis have slightly higher frequencies than the experimental modes. This is primary because the finite element uses the displacement approach in its element formulation.

More work is required to establish better ways of evaluating damping factors.

It is felt that with the expertise and equipment acquired during these tests, the normal modes of vibration of any linear helicopter structure can be efficiently derived.

REFERENCES

1. Kennedy, C. and Pancu, C. "Use of Vectors in Vibration Measurement and Analysis". Aeronautical Sciences November, 1947.
2. Meirovitch, L. "Elements of Vibration Analysis. "Mc Graw - Hill Book Company, Inc. 1975.
3. Proch, J. "Mechanical Vibration and Shock Measurements. "K. Larsen & søn A/S, Denmark, 1984.
4. Timoshenko, S., "Vibration Problems in Engineering., "John Wiley and Son, 1974.
5. Zienkiewicz, U., "The Finite Element Method in Engineering Sciences.", Mc Graw - Hill 1971.

Table 1 Theoretical and Experimental Mode Shape Comparisons

Mode No.	Mode Frequency (Hz)		Modal damping Q-Factor	Mode Shape Description
	Finite Element	Experiment		
1	6.824	6.414	36.22	Fundamental Vertical bending of Fuselage.
2	6.962	6.607	43.82	Fundamental Lateral bending of Fuselage.
3	11.760	11.395	33.15	Vertical bending of tailplane.
4	14.648	13.789	24.07	Second Vertical bending of Fuselage.
5	17.895	16.956	48.10	Fore - and - aft bending of tailplane.
6	22.485	21.299	14.25	Torsion of Fuselage
7	23.760	23.551	13.40	Engine vertically antisymmetric.
8	25.810	25.486	24.18	Engine Vertically symmetric.
9	30.100	29.905	102.50	Tailcone struts
10	33.628	33.311	90.85	Fuselage second lateral bending.
11	48.869	43.498	23.90	Second vertical bending of tailplane.

NOMENCLATURE

- F Force amplitude vector.
- H Hysteretic damping matrix.
- k Stiffness matrix.
- t Time.
- w Forcing frequency.
- w_n Normal mode natural frequency.
- $X(t)$ Time dependent displacement vector.
- $\phi(w)$ Phase lag between the response and the excitation.

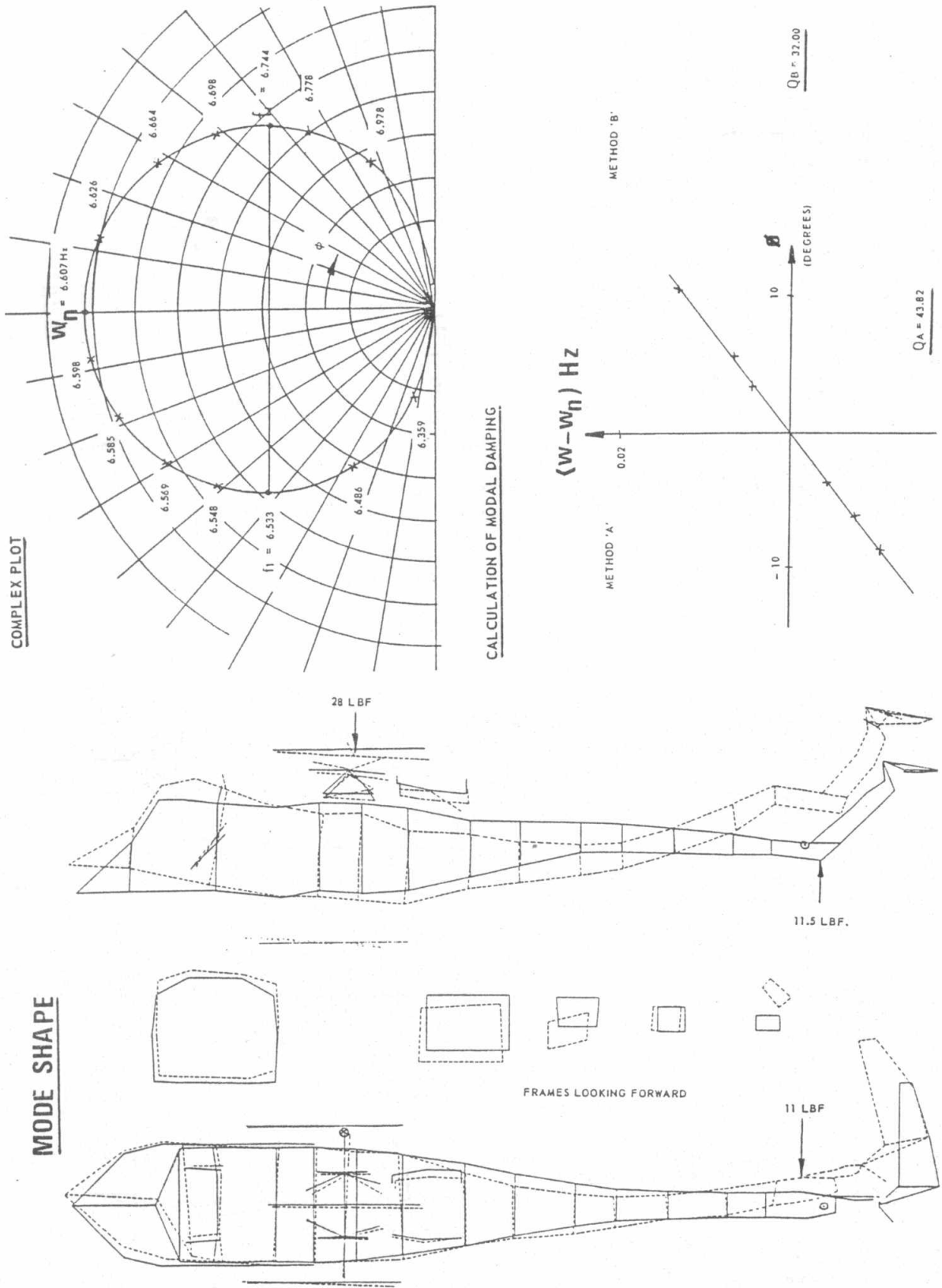


Fig. 3. Experimental normal mode N_{02} -frequency 6.607 Hz.

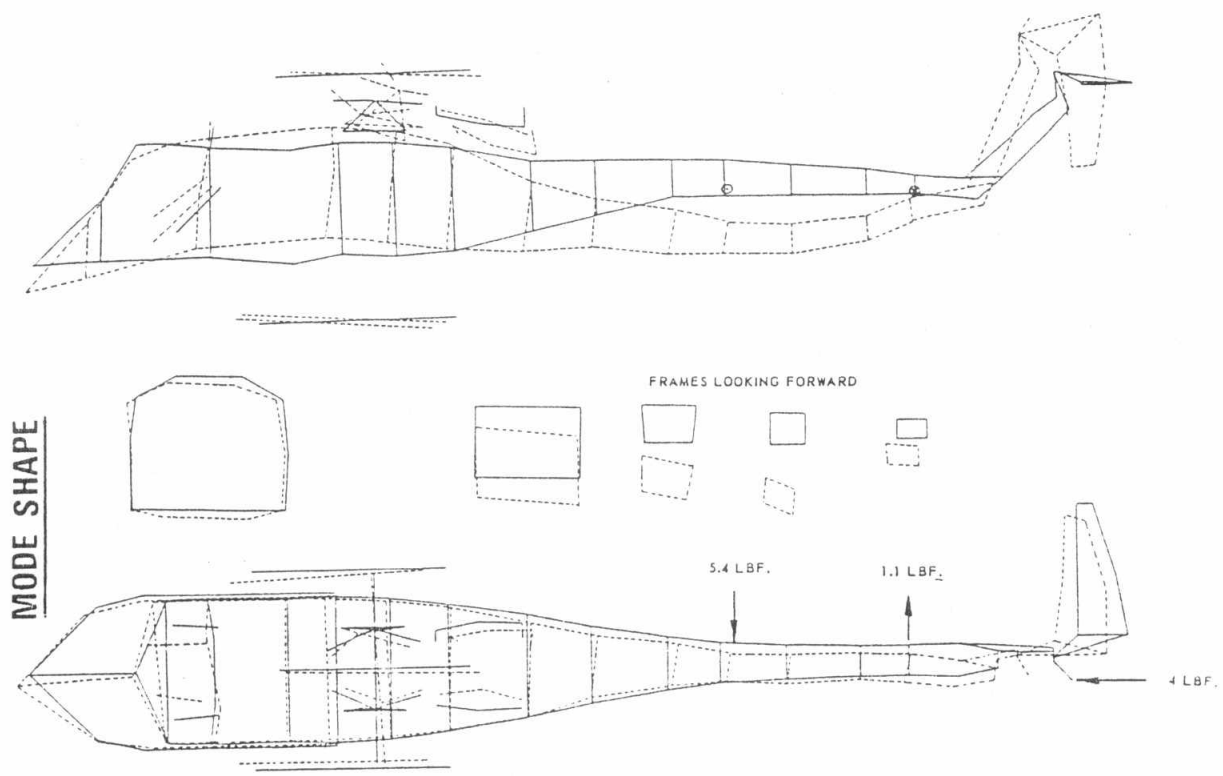
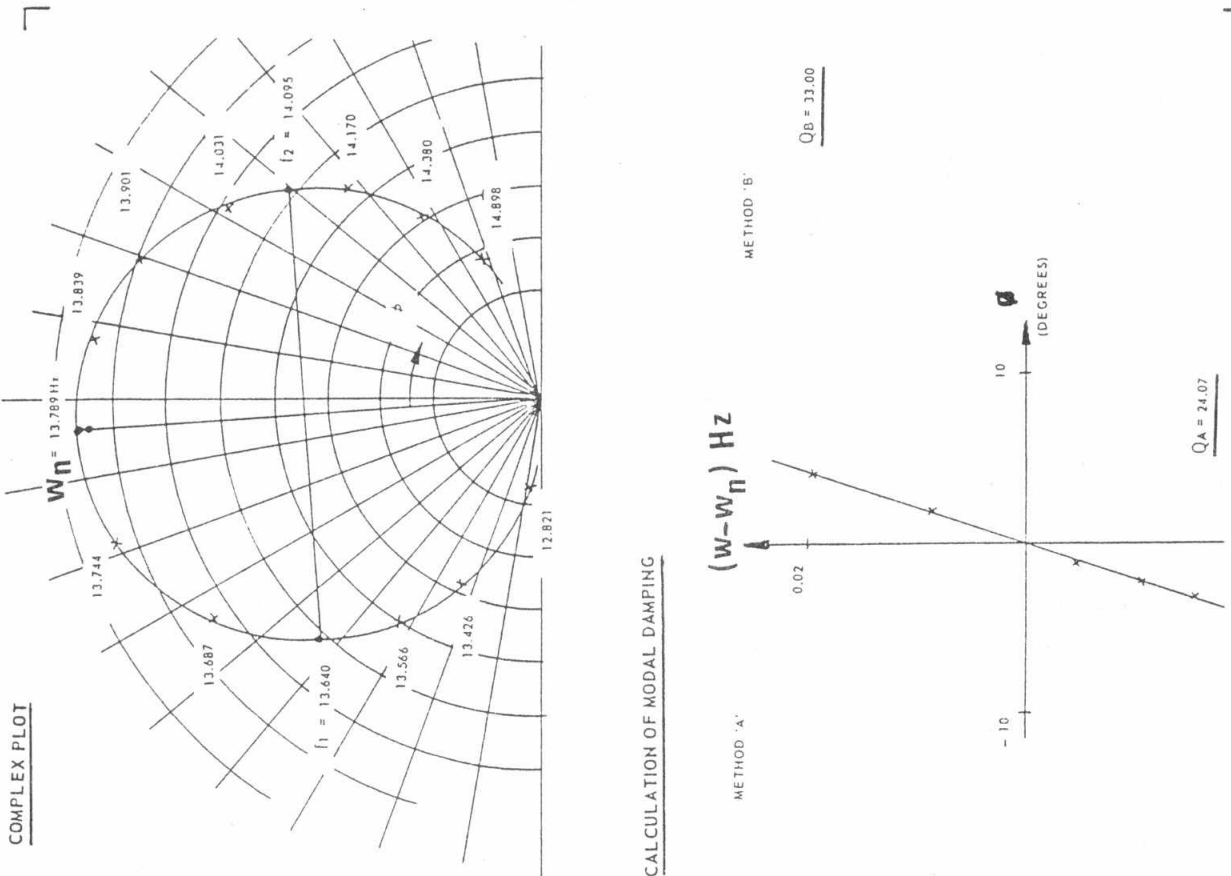


Fig. 4. Experimental normal mode No 4 - frequency 13.789 Hz.